Developmental Biology 333 (2009) 161–172

Contents lists available at ScienceDirect

Developmental Biology

journal homepage: www.elsevier.com/developmentalbiology

A role for chemokine signaling in neural crest cell migration and craniofacial development

Eugenia C. Olesnicky Killian, Denise A. Birkholz, Kristin Bruk Artinger *

Department of Craniofacial Biology, University of Colorado Denver School of Dental Medicine, Aurora, CO 80045, USA

ARTICLE INFO

Article history:
Received for publication 20 November 2008
Revised 22 June 2009
Accepted 23 June 2009
Available online 1 July 2009

Keywords:
Chemokine
cxcr4
sdf1
cxcr7
Neural crest
Migration
Neurocranium
Endoderm

ABSTRACT

Neural crest cells (NCCs) are a unique population of multipotent cells that migrate along defined pathways throughout the embryo and give rise to many diverse cell types including pigment cells, craniofacial cartilage and the peripheral nervous system (PNS). Aberrant migration of NCCs results in a wide variety of congenital birth defects including craniofacial abnormalities. The chemokine Sdf1 and its receptors, Cxcr4 and Cxcr7, have been identified as key components in the regulation of cell migration in a variety of tissues. Here we describe a novel role for the zebrafish chemokine receptor Cxcr4a in the development and migration of cranial NCCs (CNCCs). We find that loss of Cxcr4a, but not Cxcr7b, results in aberrant CNCC migration defects in the neurocranium, as well as cranial ganglia dysmorphogenesis. Moreover, overexpression of either Sdf1b or Cxcr4a causes aberrant CNCC migration and results in ectopic craniofacial cartilages. We propose a model in which Sdf1b signaling from the pharyngeal arch endoderm and optic stalk to Cxcr4a expressing CNCCs is important for both the proper condensation of the CNCCs into pharyngeal arches and the subsequent patterning and morphogenesis of the neural crest derived tissues.

Introduction

The neural crest (NC) is an evolutionarily conserved cell population among vertebrates that has long fascinated researchers due to the ability of neural crest cells (NCCs) to migrate and differentiate into a number of different cell types (LaBonne and Bronner-Fraser, 1998; Ayer-Le Lievre and Le Douarin, 1982). NCCs are induced at the border of the neural plate and the non-neural ectoderm, delaminate from the neural tube and migrate throughout the body, giving rise to various cell types including pigment cells, craniofacial cartilage and the peripheral nervous system (PNS) (Ayer-Le Lievre and Le Douarin, 1982; Brugmann et al., 2006; Huang and Saint-Jeannet, 2004; Raible et al., 1992; Kontges and Lumsden, 1996; Trainor, 2005; Trainor and Krumlauf, 2000; Schilling and Kimmel, 1994; Serbedzija et al., 1994, 1990). Cranial neural crest cells (CNCCs) migrate in three streams, with the anteriormost CNCCs emigrating first, followed by the emigration of more caudally located CNCCs. The segmental fate of the CNCCs is dictated through the premigratory position of the CNCCs along the antero-posterior axis of the embryo. Once the CNCCs reach their destination in the arches, signaling via tissue interactions between endoderm, mesoderm, ectoderm and CNCCs directs the final cell fate (Clouthier and Schilling, 2004).

The peripheral nervous system in the anterior region of the embryo consists of a series of cranial ganglia and glia that are derived from both CNCCs and ectodermal placodes. While the precise contributions of the placodes and CNCCs to many of the zebrafish cranial ganglia is not known, the trigeminal sensory ganglia are derived from both CNCCs and placodal cells (Holzschuh et al., 2005; Knaut et al., 2005; Schilling and Kimmel, 1994). Trigeminal neurons extend axonal projections throughout the head and are important for detecting chemical, mechanical and thermal stimuli (Knaut et al., 2005).

In the zebrafish embryo, CNCCs of the pharyngeal arches give rise to the ventral pharyngeal skeletal elements. Specifically, pharyngeal arch one gives rise to the Meckel's and palatoquadrate cartilages, arch two forms the basihyal, ceratohyal and hyosymplectic cartilages and arches three through seven give rise to the ceratobranchial cartilages (Schilling et al., 1996; Piotrowski et al., 1996). The dorsal craniofacial cartilages make up the neurocranium or "braincase". The anterior neurocranium is composed of two rod-like structures, termed trabeculae, which fuse anteriorly and connect to the ethmoid plate. The anterior neurocranium is derived from the anteriormost CNCCs that migrate out from the dorsal neural tube and reach the dorsal anterior aspect of the head following a path along the optic stalks, medial to the eyes (Wada et al., 2005; Eberhart et al., 2006; Langenberg et al., 2008).

Several recent studies have implicated multiple key signaling pathways in the development of craniofacial cartilages and ganglia. Previous studies have established that defects in Shh signaling in zebrafish cause aberrant neurocranium and viscerocranial development (Wada et al., 2005; Eberhart et al., 2006). Additionally, Fgf signaling from the pharyngeal endoderm is important for normal arch and subsequent cartilage development (Crump et al., 2004; Piotrowski and

* Corresponding author. Fax: +1 303 724 4580.
E-mail address: Kristin.Artinger@ucdenver.edu (K.B. Artinger).

0012-1606/$ – see front matter © 2009 Elsevier Inc. All rights reserved.
doi:10.1016/j.ydbio.2009.06.031

Nusslein-Volhard, 2000). Finally, Retinoic Acid (RA) signaling has also been shown to be important during craniofacial development, specifically for endodermal pouch morphogenesis (Kopinke et al., 2006). Thus, complex signaling interactions are required for proper development of the craniofacial skeleton. The zebrafish NC provides an outstanding model for the study of migration of diverse cell types and their subsequent differentiation. Yet while many studies have uncovered various molecular mechanisms for NCC differentiation and patterning, little is known about the signaling effectors that regulate migration of CNCCs (Yelick and Schilling, 2002).

Chemokines are small, secreted chemoattractants that have been well studied for their roles in regulating cell migration during embryogenesis, immune response and cancer (Kucia et al., 2004). The chemokine, Stromal cell derived factor (Sdf1), which preferably binds to the receptors Cxcr4 and Cxcr7 (Balabanian et al., 2005; Bleul et al., 1996; Boldajipour et al., 2008; Horuk, 2001), has been reported to regulate cell trafficking of hematopoetic stem cells (Horuk, 1998) and to promote migration of germ cells (Doitsidou et al., 2002; Thorpe et al., 2004; Dumstrei et al., 2004; Knaut et al., 2003; Molyneaux et al., 2003; Sasado et al., 2008). Recently, Boldajipour et al. (2008) have shown that during germ cell migration, Sdf1 signals through Cxcr4, while Cxcr7 instead functions as a mock receptor for Sdf1. Cxcr7 thus functions in ligand sequestration and is thought to play a role in the generation of an Sdf1 gradient that directs germ cell migration into the presumptive gonad (Boldajipour et al., 2008).

Cxcr4 has also been shown to be expressed in migrating NCCs in the mouse embryo. *Sdf1*, conversely, is expressed within the migratory path of the NCCs and has been shown in mouse to signal through Cxcr4 to mediate positioning of dorsal root ganglia (DRG) (Belmadani et al., 2005). In addition, expression analysis of *sdf1* in the chick embryo reveals an *sdf1* expression domain within the branchial arch region (Rehimi et al., 2008).

Two *cxcr4* genes, *cxcr4a* and *cxcr4b*, have been isolated in zebrafish and are closely related to mammalian *cxcr4*. Similar to mouse, zebrafish *cxcr4a* is expressed within NCCs (Chong et al., 2001). Although a functional analysis of the *cxcr4* genes in NCC migration has not been reported for zebrafish, *cxcr4b* has been shown to be important for proper positioning of the partially NC-derived trigeminal sensory ganglia (Knaut et al., 2003). Moreover, Sdf1a signaling has been implicated in melanophore patterning of the zebrafish embryo, suggesting a link between Sdf1–Cxcr4 signaling and NC migration (Svetic et al., 2007). Here we describe a new role for *cxcr4a* and *sdf1b*, but not *cxcr7b*, in CNCC migration and patterning during zebrafish craniofacial development.

Materials and methods

Animals

The zebrafish were maintained according to Westerfield (1993) and staged by hours post fertilization and morphology according to Kimmel et al. (1995). ntl^{b195} and flh^{n1} mutant lines were obtained from the Zebrafish International Resource Center.

Embryo manipulation and analysis

Whole-mount *in situ* hybridization was adapted from Thisse and Thisse (1998) and Brent et al. (2003) (Brent et al., 2003). Double fluorescent *in situ* hybridization was performed as described by Pineda et al. (2006). Immunohistochemistry was performed as described (Ungos et al., 2003). anti-Zn8 primary antibody (ZIRC) was used at a 1:25 dilution. Anti-HuC/D (Molecular Probes) was used at a 1:1000 dilution. Alcian blue staining was performed as described (Schilling et al., 1996).

For live imaging, 12 hpf embryos were mounted in 0.7% low melt agarose in fish water and oriented in a dorso-lateral angle. CNCC migration was followed using a Zeiss LSM 510 confocal microscope equipped with a heated stage set to 28 °C. Z stack images were taken once every 5 min. Double *in situ* hybridizations were visualized using Zeiss LSM 510 confocal microscope. Quantification of expression overlap was preformed using Zeiss Meta software. The colocalization coefficients were calculated based on the relative number of pixels that overlap, expressed over the total number of pixels for a value of 0 (not colocalized) to 1 (colocalized). *cxcr4a* expression with neural crest cell markers (*barx1*, *dlx2a*, *hand2*, *crestin*), and both *sdf1b* and *cxcr7b* with the endodermal marker *nkx2.3* have 0.9–1 colocalization coefficients, showing regions of pixel overlap.

Sections were completed following embedding of embryos in either 1.5% agar in 5% sucrose or in OCT and were sectioned using a cryostat for a thickness between 9–12 μm.

Antisense Morpholino oligonucleotide injections

Antisense Morpholino Oligonucleotide (MO) for *cxcr4a*, *cxcr7b* and *sdf1b* has been previously described: *cxcr4a* MO1 5′-ATAAGCCATCTC-TAAAAGACTTCTC-3′; *cxcr4a* mismatch MO 5′-ATAAACCATATCTAAGA-GACGTCT-3′; *cxcr4a* MO3 5′-GACTTCTCCCGTTCCTTCAGTCTCC-3′ (Chong et al., 2007);*sdf1b* 5′-CGCTACTACTTTGCTATCCATGCCA-3′(Knaut et al., 2005); *cxcr7b* 5′-TCATTCACGTTCACACTCATCTTGG-3′ (Dambly-Chaudiere et al., 2007). Universal Control MO sequence: 5′-CCTCTTACCTCAGTTA-CAATTTATA-3′. The oligonucleotides were dissolved in distilled water. *cxcr4a* MO3 or *cxcr4a* MO1 were injected into 1- to 4-cell-stage embryos together with rhodamine dextran (Molecular Probes). Universal control Morpholino and *cxcr4a* mismatch Morpholinos did not result in any craniofacial phenotypes. *cxcr4a* MO1 and *cxcr4a* MO3 gave similar craniofacial phenotypes.

DNA constructs and RNA overexpression

For overexpression, the *cxcr4a* or *sdf1b* ORF was cloned into the pCS2 vector. RNA was prepared using the mMessage mMachine capped RNA transcription kit (Ambion). Capped RNA was injected into 1-cell-stage embryos together with rhodamine dextran (Molecular Probes).

Results

The chemokine receptors cxcr4a and cxcr7b are expressed within the pharyngeal arches

Previous work has shown that the chemokine receptor *cxcr4* is expressed in the trunk NC in mouse embryos and is important for proper DRG positioning (Belmadani et al., 2005). We asked whether (1) *cxcr4* has a conserved expression pattern within the NC among vertebrates and (2) if *cxcr4* is required for NCC migration in the zebrafish embryo. We first analyzed the expression patterns of both *cxcr4a* and *cxcr4b* during zebrafish embryonic development. At 14–17 h post fertilization (hpf), when CNCCs are migrating, *cxcr4b* mRNA is not expressed in the NC (data not shown; (Chong et al., 2001), whereas *cxcr4a* is expressed within the cranial NCCs but not in trunk NCCs of the embryo (Figs. 1A, B) (Chong et al., 2007, 2001). At 17 hpf, *cxcr4a* is also expressed in the region of the optic stalk (Fig. 1B; arrow, inset shows higher magnification view) and by 24 hpf, *cxcr4a* is expressed both in the optic stalk region (Fig. 1C, arrow) and throughout the pharyngeal arches. We do however note that *cxcr4a* is excluded from the central region of arch 1, which may correspond to the mesodermal core (Fig. 1C). Although we also observe this core upon sectioning, we cannot completely rule out the possibility that *cxcr4a* is expressed at low levels in the mesodermal core. At 25 hpf, as the pharyngeal arches begin to condense into distinct structures, *cxcr4a* expression begins to form discrete expression domains that correspond to the pharyngeal arches (Fig. 1D). By 36 hpf, *cxcr4a*

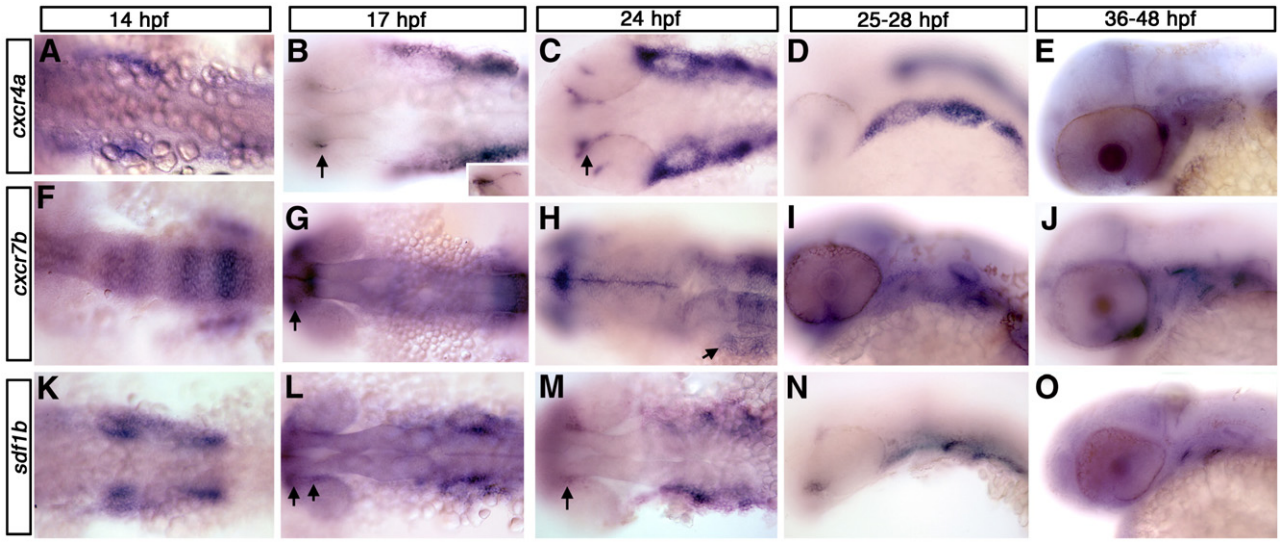

Fig. 1. *cxcr4a*, *cxcr7b*, and *sdf1b* expression in the zebrafish embryo. Dorsal views (A, B, C, F, G, H, K, L, M), lateral views (D, E, I, J, N, O) and anterior to the left. (A–E) *cxcr4a* expression. *cxcr4a* is observed in NCCs migrating to the arches (A). At 17 hpf (B) and 24 hpf (C) is expressed in the optic stalk (B, C; arrows) and pharyngeal arch region but is excluded from the central arch, likely corresponding to the mesodermal core. By 25 hpf, *cxcr4a* expression condenses into discreet arches (D). At 36 hpf, *cxcr4a* is expressed in the optic stalk and throughout the arches (E). (F–J) *cxcr7b* expression. From 14–17 hpf, *cxcr7b* is expressed in the midbrain, otic placode and in rhombomeres 3, 5 and 6 and, at 17 hpf, in the optic stalk (F, G; arrow in G to optic stalk). By 24 hpf, *cxcr7b* is expressed in the ventral region of the posterior pharyngeal arches (H, arrow). From 28–48 hpf, *cxcr7b* expression is seen throughout the pharyngeal arches (I, J). (K–O) *sdf1b* expression. At 14–17 hpf, *sdf1b* is expressed in the region of the migrating CNCCs, within the optic stalk and dorsal rim of eye (K, L; arrows in L and M). By 24 hpf (M) *sdf1b* is expressed in the typical scalloped pattern of the pharyngeal endoderm. At 25 hpf, *sdf1b* is expressed in endodermal pouches 1–3 (N) and pouches 1 and 2 at 36 hpf (O).

expression is prominent in the optic stalk (Chalasani et al., 2007; Li et al., 2005) and at a lower level throughout the arches (Fig. 1E).

Recent reports have shown that the chemokine *sdf1* binds both *cxcr4* and *cxcr7* chemokine receptors, although *cxcr7* functions as a mock receptor (Balabanian et al., 2005; Boldajipour et al., 2008; Horuk, 2001). Moreover, *cxcr7* and *cxcr4* genes function together to guide germ cells to the presumptive gonad (Sasado et al., 2008) and to guide migration of the lateral line during zebrafish development (Dambly-Chaudiere et al., 2007; Valentin et al., 2007). We therefore analyzed the expression pattern of *cxcr7b* throughout the development of the zebrafish embryo to ascertain whether or not *cxcr4a* and *cxcr7b* are similarly expressed in the pharyngeal arches. From 14–17 hpf, *cxcr7b* is expressed in the midbrain, the region surrounding the otic placode, optic stalk and in rhombomeres 3, 5 and 6 (Figs. 1F, G; arrow) but is not expressed in the CNCCs at these early stages. By 24 hpf, *cxcr7b* is expressed in the posterior arch region, ventral to the otic vesicle (Fig. 1H; arrow) and from 28–48 hpf is expressed throughout the pharyngeal arches (Thisse et al., 2001) (Figs. 1I, J). Taken together, the results of the expression analysis show that both *cxcr4a* and *cxcr7b*, but not *cxcr4b*, are expressed in the pharyngeal arch region. However, the expression patterns of these chemokine receptors within the pharyngeal region are distinct from one another suggesting they may function within different tissues.

The chemokine Sdf1b is expressed in the pharyngeal endoderm

We next examined the expression patterns of the Cxcr4 receptor ligands *sdf1a* and *sdf1b* to determine if they might function with *cxcr4a* in CNCC development. We did not detect *sdf1a* in the CNCC (data not shown; Thisse et al., 2001), but found *sdf1b* expressed within the domain of CNCC migration from 14–17 hpf, as has been previously described (Chong et al., 2007) (Figs. 1K, L). At 17 hpf, *sdf1b* is also expressed within the optic stalk region and along the dorsal rim of the eye (Fig. 1L, arrows). At 24 hpf, *sdf1b* is expressed in the optic stalk (Fig. 1M, arrow) and in a scalloped pattern that is typical of the endoderm of the pharyngeal arches (Fig. 1M). As pharyngeal arch development proceeds, the pharyngeal endoderm migrates laterally to form pouches that interdigitate each of the pharyngeal arches (Crump et al., 2004). Between 25–36 hpf, *sdf1b* is seen in pharyngeal endodermal pouches 1, 2 and faintly in pouch 3 (Figs. 1N, O). Previous studies have also shown that *sdf1b* is expressed posterior and dorsal to the optic chiasm at 48 hpf and functions in retinal axon guidance (Chalasani et al., 2007; Li et al., 2005). We note, however, that expression of *sdf1b* is already evident in the region of the optic stalk by 17 hpf (Fig. 1L, arrows). Importantly, it has been reported that anterior CNCCs travel along the dorsal optic vesicle to populate the region that will give rise to the neural crest derived anterior neurocranium (Wada et al., 2005; Eberhart et al., 2006; Langenberg et al., 2008).

Signaling between various tissue types including ectoderm, CNCCs and endoderm is integral to proper pharyngeal arch development (Graham and Smith, 2001; Knight et al., 2005; Piotrowski and Nusslein-Volhard, 2000). In order to rule out the possibility that *sdf1b* and *cxcr4a* are also expressed within the ectoderm, we prepared transverse and sagittal cryosections through the pharyngeal arch region of 25 hpf embryos that were labeled by *in situ* hybridization for *sdf1b* and *cxcr4a* mRNA. From this analysis, we find that neither *sdf1b* nor *cxcr4a* are expressed in the ectoderm within the pharyngeal arch region, although we cannot rule out the possibility that there is expression that is not detectable by *in situ* hybridization (Supplemental Fig. S1).

cxcr4a is expressed in the CNCC of the pharyngeal arches

We next performed additional expression analyses to determine which tissues *cxcr4a*, *sdf1b* and *cxcr7b* are expressed in during pharyngeal arch morphogenesis. To determine whether *cxcr4a*, *cxcr7b* or *sdf1b* are expressed in the NC of the pharyngeal arches, we performed double fluorescent *in situ* hybridization (Pineda et al., 2006) using the CNCC marker *dlx2a*, which is expressed throughout the pharyngeal arch NC (Kimmel and Eberhart, 2008). *cxcr4a* has been reported to be expressed in CNCCs in zebrafish during CNCC migration (Chong et al., 2001). We find that *cxcr4a* and the neural crest marker *dlx2a* partially overlap in the anterior arches at 25 hpf after CNCC migration has ceased (Figs. 2A–C, arrow). We also find that *sdf1b* and *cxcr7b* are not coexpressed with *dlx2a* in the anterior arches. *cxcr7b* is, however, coexpressed in a small subset of *dlx2a* positive cells within

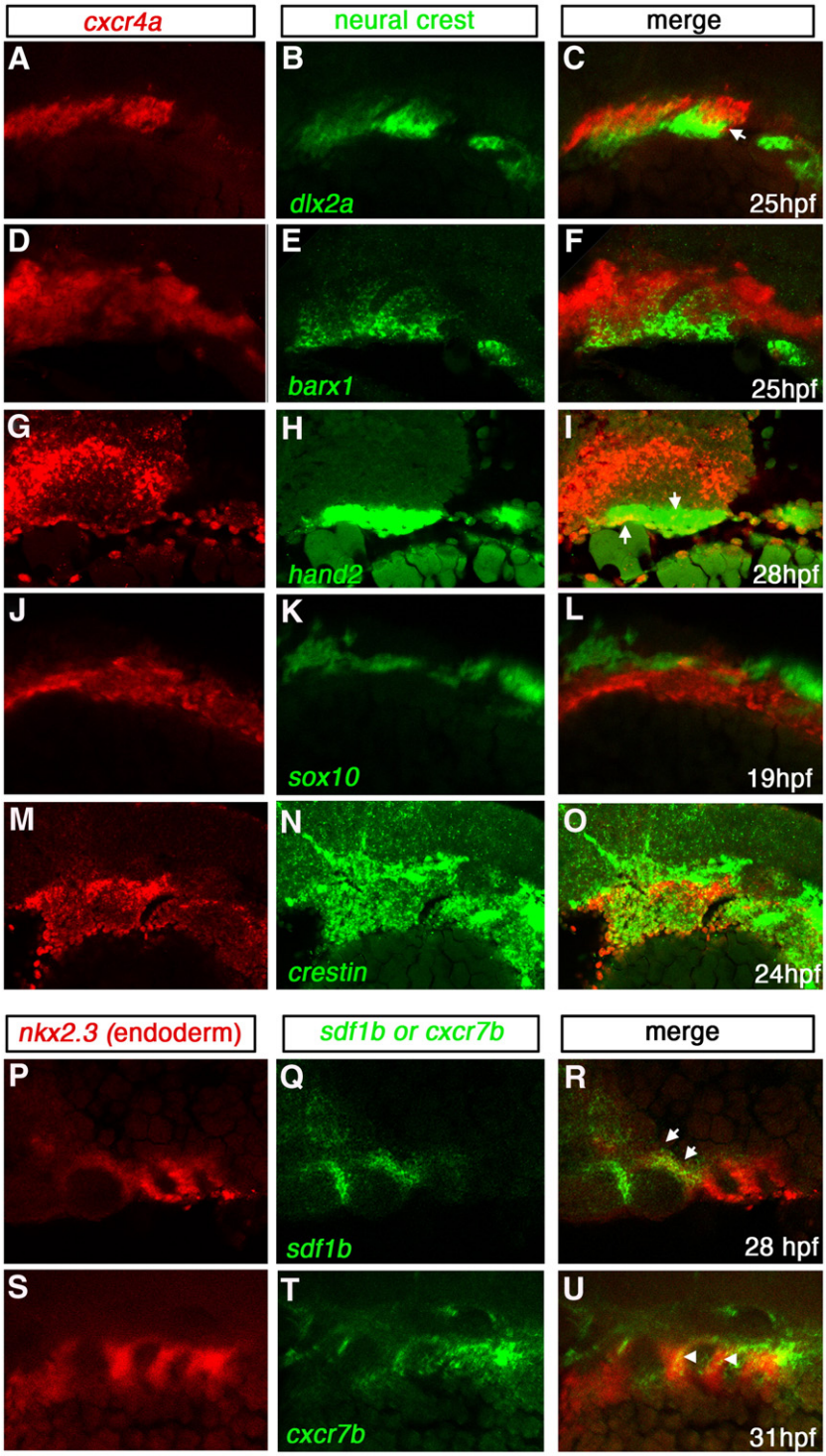

Fig. 2. Expression of *cxcr4a*, *cxcr7b* and *sdf1b* in the developing pharyngeal arches. Lateral views, anterior to the left. Single channel (A, B, D, E, G, H, J, K, M, N, P, Q, S, T) and merged (C, F, I, L, O, R, U) images of confocal micrographs of double fluorescent *in situ* hybridization of *cxcr4a*, *cxcr7*, and *sdf1b* along with tissue specific marker expression in the pharyngeal arch region. Neural crest markers are indicated in green with *cxcr4a* (red) in A–O, and endodermal marker *nkx2.3* (red) with *sdf1b* or *cxcr7b* (green) in P–U. (A–C) CNCC marker *dlx2a* expression (green) overlaps *cxcr4a* (red) in a subset of CNCCs (yellow, arrows) at 25 hpf. (D–F) *barx1* is coexpressed in a subset of *cxcr4a* cells at 25 hpf. (G–I) At 28 hpf, *hand2* is expressed in the ventral-most domain of arch CNCCs and partially overlaps with *cxcr4a* in this domain (yellow, arrows). (J–L) *cxcr4a* (red) is mostly excluded from *sox10* nonectomesenchymal expression at 19 hpf (green). (M–O) The pan CNCC marker *crestin* is expressed in a broad domain in the pharyngeal arch region, where *cxcr4a* is also expressed. *cxcr4a* is excluded from the dorsal *crestin* domain that corresponds to nonectomesenchymal NCCs. (P–R) *sdf1b* (green) and the endodermal marker *nkx2.3* (red) overlap in pouch 2 (arrows) at 28 hpf. (S–U) *cxcr7b* (green) is coexpressed with *nkx2.3* (red) throughout pharyngeal arch endoderm at 31 hpf (yellow; arrowheads).

the posterior arches (Supplemental Figs. S2J–L; data not shown). Moreover, *cxcr7b* is expressed in cells that surround and interdigitate each of the *dlx2a* positive pharyngeal arches at 28 hpf (Supplemental Figs. S2J–L); this pattern is similar to the expression of markers known to be expressed in the pharyngeal endoderm.

We next examined whether *cxcr4a* colocalizes with *barx1*, which is expressed in the pharyngeal arch NC (Sperber and Dawid, 2008). We find that at 25 hpf *barx1* is coexpressed in a subset of NCCs with *cxcr4a* in the anterior pharyngeal arches. This colocalization is restricted to the ventral and medial portion of the arches but not to

the dorsal region of the arches where *barx1* expression is absent. We also note that *cxcr4a* is expressed in a region dorsal to the arches between arches 2 and 3, which does not correspond to the pharyngeal arch crest (Figs. 2D–F). In order to confirm the exact boundaries of *barx1* expression within the pharyngeal arch crest, we examined the colocalization of *barx1* and *dlx2a* at 25 hpf. Consistent with our findings regarding the colocalization of *barx1* and *cxcr4a*, we find that in the anterior arches, *barx1* expression is excluded from the dorsal domain of *dlx2a* but is coexpressed in the medial and ventral domain of *dlx2a* expression (Supplemental Figs. S2M–O). *hand2* is expressed in CNCCs that reside in the ventral-most region of the pharyngeal arches (Miller et al., 2003). Consistent with the expression results with *barx1*, we find that *cxcr4a* and *hand2* partially overlap in the ventral-most CNCCs of the anterior pharyngeal arches at 28 hpf (Figs. 2G–I; arrows).

In order to ascertain whether *cxcr4a* is also expressed in the nonectomesenchymal CNCCs that give rise to the cranial ganglia and glia, we examined whether or not *cxcr4a* is coexpressed with the nonectomesenchymal NC marker *sox10* during pharyngeal development (Blentic et al., 2008). We find that at 19 hpf *cxcr4a* is excluded from the *sox10* expression domain in the anterior stream but does colocalize with a small subset of *sox10* expressing cells midway between the eye and otic vesicle (Figs. 2J–L). We next examined whether *cxcr4a* colocalizes with the pan-NC marker *crestin*. At 28 hpf, *cxcr4a* and *crestin* are partially colocalized throughout the anterior pharyngeal arch crest, but *cxcr4a* is excluded from the nonectomesenchymal NC, located dorsal to the anterior arches (Figs. 2M–O). Taken together, these results show that *cxcr4a* is expressed throughout CNCC migration and this expression persists within the CNCCs of the anterior pharyngeal arches post-migration, during pharyngeal arch condensation and patterning.

sdf1b and cxcr7b are expressed in the pharyngeal endoderm

In order to determine whether *sdf1b* and *cxcr7b* are expressed in the endoderm, we performed double fluorescent *in situ* hybridization using the endodermal marker *nkx2.3*. We find that *sdf1b* is coexpressed with *nkx2.3* in pharyngeal pouch 2 (Figs. 2P–R; arrows). Moreover, while *nkx2.3* is only weakly expressed in pouch 1, *sdf1b* is strongly expressed in the first pouch. Additionally, *cxcr7b* is partially coexpressed with *nkx2.3* in the pharyngeal arch endoderm (Figs. 2S–U; arrowheads). These results indicate that *cxcr7b* and *sdf1b* are expressed in the pharyngeal endoderm.

cxcr4a, cxcr7b and sdf1b expression within the pharyngeal arches

We next sought to determine whether the expression of these chemokine receptors and *sdf1b* might overlap using double fluorescent *in situ* hybridization analyses. *sdf1b* and *cxcr4a* are expressed in a complementary manner at 25 hpf, with only a subset of coexpressing cells at the border of the endoderm and arch crest (Supplementary Figs. S2A–C). Conversely, we find that *cxcr7b* and *sdf1b* are coexpressed in both the medial endoderm and within the first 3 pharyngeal pouches at 28 hpf (Supplementary Figs. S2D–F). At 28 hpf, *cxcr4a* and *cxcr7b* are not coexpressed within the endoderm, but do show coexpression in a small subset of cells within the posterior arches (Supplementary Figs. S2G–I).

In summary, these results indicate that *cxcr4a* is expressed predominantly in the anterior pharyngeal arch CNCCs, while *sdf1b* and *cxcr7b* are expressed predominantly in the endoderm during pharyngeal arch development. This is consistent with previous studies that have shown that the chemokines *sdf1a* and/or *sdf1b* are often expressed in adjacent and complementary tissues to *cxcr4a* or *cxcr4b* expressing domains (Li et al., 2005; Schwarting et al., 2006; Miyasaka et al., 2007; Chalasani et al., 2007).

Loss of Cxcr4a signaling results in neurocranium defects

The expression of *cxcr4a* in the arch neural crest during pharyngeal arch development and within the optic stalk suggests that *cxcr4a* might function in the development of the ventral and dorsal craniofacial cartilages. In order to investigate the function of Cxcr4a in craniofacial development, we used Morpholino-mediated depletion of the *cxcr4a* gene product (Chong et al., 2007). We utilized 2 Morpholinos designed to knockdown *cxcr4a,* a control mismatch Morpholino (Chong et al., 2007) and a universal control Morpholino to verify specificity of the *cxcr4a* Morpholinos. We find that both *cxcr4a* Morpholinos result in similar craniofacial phenotypes (described below), whereas, even high doses (up to 25 ng) of the control mismatch and universal control Morpholino do not result in any craniofacial phenotypes. Moreover, when *cxcr4a* mRNA is coinjected with either *cxcr4a* Morpholino, the craniofacial phenotype is partially rescued (Table 1). Taken together, these results indicate that the *cxcr4a* Morpholinos are specific for *cxcr4a* mRNA.

At 6.5 dpf, *cxcr4a* morphants have reduced forebrains as compared to wildtype and control Morpholino injected embryos, resulting in a "dolphin-like" appearance (Supplementary Figs. S3G, H). We performed alcian blue staining to visualize the cartilage of these morphant larvae. While disrupting Cxcr4a signaling does not result in defects in the ventral pharyngeal skeleton, we find that the ethmoid plate is severely reduced or absent and that the trabeculae of the neurocranium are fused and thickened (Figs. 3A, B). This reduction in the neurocranium accounts for the "dolphin-like" appearance of *cxcr4a* morphants.

If Sdf1b and Cxcr7b function with Cxcr4a in its role in craniofacial development, then knockdown of *sdf1b* and *cxcr7b* should result in a similar phenotype to *cxcr4a* morphants. Indeed we find that *sdf1b* morphants phenocopy the craniofacial defects seen in *cxcr4a* morphants, and have additional defects in anterior basicapsular commissure formation (Fig. 3C, arrow). Knock down of *cxcr7b* however, does not result in craniofacial defects (data not shown). These results suggest that Sdf1b and Cxcr4a function together in development of the neurocranium.

Although both *cxcr7b* and *cxcr4a* are expressed in the pharyngeal arches, knockdown of either gene surprisingly does not result in ventral craniofacial cartilage defects. To rule out the possibility that these genes might function redundantly with one another during morphogenesis of the pharyngeal skeleton, we performed double knockdown of *cxcr7b* and *cxcr4a* and analyzed the resulting cartilage phenotype. *cxcr4a* and *cxcr7b* double morphants do not have a phenotype within the pharyngeal skeleton, suggesting they do not function redundantly with one another during pharyngeal arch morphogenesis (not shown).

In order to ascertain whether *cxcr4b* might also play a role in craniofacial development, we performed alcian blue staining on the *cxcr4b* mutant, *odysseus* (*ody*) at 5 dpf (Knaut et al., 2003). We find that *ody* mutants have normal craniofacial patterning, suggesting that

Table 1
Quantification of results from migration, alcian blue and *in situ* hybridization analyses in *cxcr4a* morphant embryos.

Injection	Cartilage phenotype		
	Ethmoid plate reduced	Hyposympletic defects	Ectopic
cxcr4a Morpholino (MO) (ng/nl)	26/65 (40%)		
cxcr4a MO (as control for rescue)	21/52 (40%)		
cxcr4a/*cxcr7b*[a] Morpholino (ng/nl)	37/64 (54%)		
sdf1b Morpholino (ng/nl)	30/53 (56%)		
cxcr4a mRNA overexpression	16/62 (26%)	22/62 (35.5%)	13/62 (21%)
cxcr4a Morpholino + *cxcr4a* mRNA (200 pg) rescue	11/42 (26%)		6/42 (14%)

[a] *cxcr7b* morphants alone have no craniofacial phenotype.

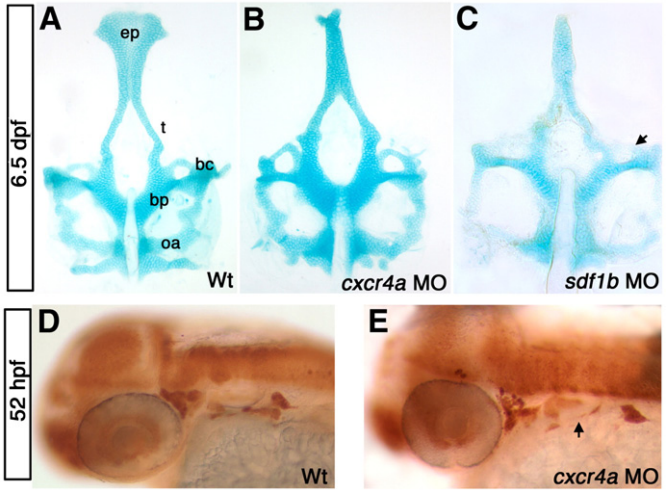

Fig. 3. *cxcr4a* morphants have neurocranium defects. Dorsal views, anterior to the top (A–C) and lateral views, anterior to the left (D, E). (A) wild type (WT) neurocranium at 6.5 dpf. (B) *cxcr4a* morphants lack an ethmoid plate (ep) and have fused trabeculae (t). (C) *sdf1b* morphants phenocopy *cxcr4a* morphants, and have more severe anterior basicapsular commissure defects (arrow). (D, E) Wildtype (D) and *cxcr4a* morphant embryo (E) labeled with anti HuC/D 52 hpf to indicate the cranial ganglia. Morphant embryos have a reduction in cranial ganglia IX and X (arrow). bc, basicapsular commissure; bp, basil plate; oa, occipital arch; ep, ethmoid plate; t, trabeculae.

cxcr4b does not play a role in craniofacial development (data not shown). This observation is supported by absence of *cxcr4b* expression within CNCCs and pharyngeal arches (Chong et al., 2001).

Two recent reports by Nair and Schilling (2008) and Mizoguchi et al. (2008) show that *cxcr4a* is important for endodermal cell migration during zebrafish gastrulation. The studies show that impaired Cxcr4a signaling leads to aberrant endodermal cell migration during gastrulation. Moreover, while Nair and Schilling report duplication of endodermal organs in morphants, Mizoguchi et al. report loss or reduction of these endodermal organs (Mizoguchi et al., 2008; Nair and Schilling, 2008). In order to rule out the possibility that endodermal duplications as reported by Nair and Schilling (2008) for *cxcr4a* morphant embryos can cause craniofacial defects similar to *sdf1b*/*cxcr4a* morphants, we analyzed the craniofacial skeletons of *notail* (*ntl*) and *floating head* (*flh*) mutant larvae, which also display endodermal duplications (Chen et al., 2001). We find that neither *ntl* nor *flh* mutant larvae have defects in the craniofacial skeleton that are similar to *sdf1b* or *cxcr4a* morphants (Supplementary Fig. 9). Both mutants have overall smaller heads and thus the skeletal elements are reduced in size. Additionally, both mutant lines show loss of the more posterior ceratobranchial cartilages. The dorsal skeleton, however, including the ethmoid plate and trabeculae appear normal (Supplementary Fig. S9). Thus, we find that neither *ntl* nor *flh* mutant larvae phenocopy the craniofacial defect observed in the *sdf1b* or *cxcr4a* morphants, suggesting that the craniofacial phenotypes associated with *sdf1b*/*cxcr4a* knockdown are not a consequence of early endodermal migration defects.

cxcr4a morphants have reduced cranial ganglia

Trigeminal sensory neurons have been shown to express *cxcr4b* during development (Knaut et al., 2005). Moreover, assembly of trigeminal neurons into a single ganglion cluster is mediated through signaling by Sdf1a and Sdf1b through Cxcr4b. In the absence of *sdf1a*, *sdf1b* or *cxcr4b,* the trigeminal neurons form two ganglion clusters instead of a single bilateral cluster (Knaut et al., 2005).

We reasoned that since *cxcr4a* is expressed in the CNCCs and is important for CNCC migration, cranial ganglia might also be affected in the absence of *cxcr4a* signaling. We therefore analyzed the cranial ganglia in morphants at 52 hpf using antibodies against HuC/D, which is expressed in all differentiated neurons. At 52 hpf, we find that cranial ganglia IX and X are often reduced or missing in *cxcr4a* morphants (Figs. 3D, E; arrow). Conversely, *cxcr7b* morphants do not have defects in posterior cranial ganglia development (data not shown). These results suggest that *cxcr4a* is important for the development of cranial ganglia IX and X.

cxcr4a morphants have disorganized pharyngeal arches

cxcr4a is expressed in the CNCCs during migration, while *sdf1b* is expressed in the migratory pathway of CNCCs (Chong et al., 2001, 2007) from 12–20 hpf. Moreover, after CNCC migration is complete (between 20–21 hpf), *cxcr4a* and *sdf1b* are expressed within the pharyngeal arches. We therefore asked whether *cxcr4a* morphants display normal arch morphology by examining pharyngeal arches of *cxcr4a* morphants at 28 hpf in a tg{fli1::eGFP} background. tg{fli1::eGFP} is expressed in postmigratory CNCCs and the developing vasculature of the embryo (Lawson and Weinstein, 2002). While *cxcr4a* morphants have overall normal forming arches, they do however have loose and disorganized anterior arch structure as compared to the condensed arches of control siblings. In morphant embryos, the stomodeum is not well defined and CNCCs appear within the region of pharyngeal pouch 1, which normally creates a separation between arches 1 and 2 (Fig. 4 compare A, C with B; arrowheads mark

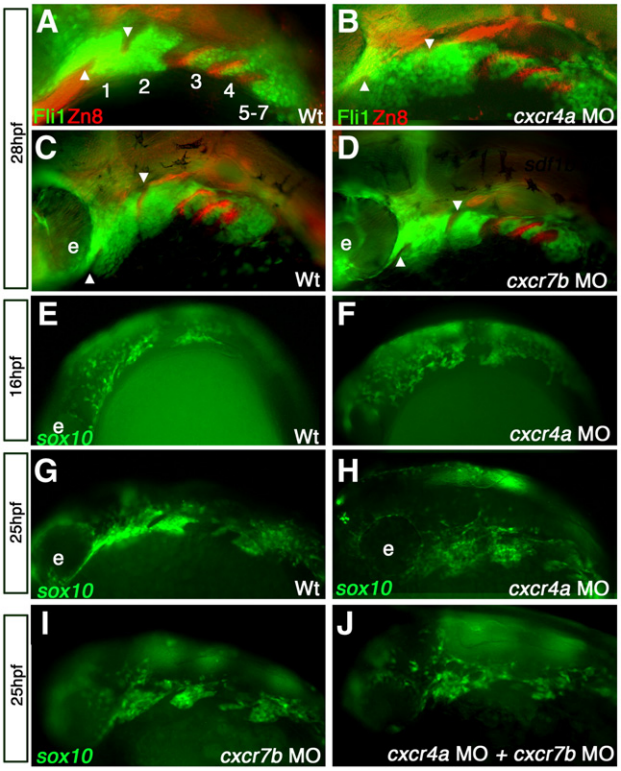

Fig. 4. *cxcr4a* morphants have aberrant CNCC migration and arch condensation. Lateral views, anterior to the left. (A–D) tg{*fli1*::eGFP} (green) embryo marking postmigratory CNCCs double labeled with the endoderm marker Zn-8 (red). (E–J) tg{*sox10*::eGFP} (green) labeling neural crest migration and condensation into the pharyngeal arch region. (A, B) *cxcr4a* morphants (B) show loose arch structure, as compared to wild type embryos. (A) Arrowheads mark endodermal pouch 1 and stomodeum in A–D as a reference for compaction. In addition, endodermal specification and morphogenesis is unaffected as seen by Zn8 expression (red). (C, D) *cxcr7b* MO injected embryos (D) have normal CNCC (green) compaction in the pharyngeal arch and endodermal expression of Zn8 (red) as compared to wildtype at 28 hpf (C). (E, G) Wildtype tg{*sox10*::eGFP} embryos display normal onset of CNCC migration from the neural tube toward the ventral arch region, migrate normally mid-migration at 16 hpf (E) and are properly organized post-migration at 25 hpf (G). Early to mid CNCC migration is unaffected in *cxcr4a* morphants at 16 hpf, as CNCCs are migrating ventrally from the neural tube (F) but show loose organization of CNCC in the anterior arches at 25 hpf (H). *cxcr7b* morphant embryos have normal arch morphology (I) and double *cxcr4a* and *cxcr7b* morphants (J) show a similar disorganized arch phenotype as *cxcr4a* single morphants.

position of endodermal pouch 1 and stomodeum; $n = 24/42$ or 57% affected). Conversely, we find that *cxcr7b* morphants have properly condensed arches at 28 hpf (Fig. 4D). This suggests that Cxcr4a, but not Cxcr7b, is involved in NCC compaction into the pharyngeal arches.

As signaling between tissues is important in pharyngeal arch development, we next asked whether endodermal pouch formation is normal in *cxcr7b*, *cxcr4a* and *sdf1b* morphants using the endoderm marker Zn8. We find that *cxcr7b*, *cxcr4a* and *sdf1b* morphants are capable of forming endodermal pouches (Figs. 4A–D red; data not shown). Thus although *sdf1b* and *cxcr7b* are expressed in the pharyngeal endoderm, they do not play a role in endoderm specification or morphogenesis of the endodermal pouches.

Since *cxcr4a* morphants display disorganized cells within the arches and *cxcr4a* is expressed in the CNCCs during migration, we asked whether CNCC migration is affected in morphants using a tg{sox10::GFP} reporter, which is expressed in migrating NCCs (Carney et al., 2006). At 16 hpf, CNCCs in *cxcr4a* morphant embryos are capable of initiating migration and NCCs are seen migrating ventrally from the dorsal neural tube into the pharyngeal arch region (Figs. 4E, F). At 25 hpf, however, morphant CNCCs appear loosely organized and more spread out in the pharyngeal arches, as compared to control siblings, in which CNCCs have begun to condense into clearly distinguishable arches (Figs. 4G, H; $n = 25/37$ or 68% affected).

We next asked whether *cxcr7b* knockdown also results in disorganized pharyngeal arches using a tg{sox10::GFP} reporter. We find that *cxcr7b* morphants have normal arch morphology at 25 hpf (Fig. 4I). Since *cxcr7b* expression within the arches does not commence until well after the NCCs have reached the arches, it is not surprising that *cxcr7b* is not necessary for establishing the general structure of the pharyngeal arches. Moreover, knocking down both *cxcr4a* and *cxcr7b* simultaneously results in a phenotype similar to *cxcr4a* single morphants (Fig. 4J). These results suggest that *cxcr7b* is dispensable for pharyngeal arch development, while *cxcr4a* is important for the formation of discrete pharyngeal arches.

cxcr4a morphants have CNCC migration defects

We next followed migration of CNCCs using time lapse confocal microscopy in wild type embryos and *cxcr4a* morphants using a tg{sox10::GFP} reporter line. We followed CNCCs from the onset of migration until after the CNCCs have condensed into the arches. We find that although *cxcr4a* morphant CNCCs are capable of initiating migration from the neural tube, CNCCs migrate to ectopic sites in the embryo (Figs. 5E–J; Supplementary movies 1 and 2). For example, we find that while in wild type control embryos, CNCCs avoid the eye during the early stages of CNCC migration (Figs. 5A–D) (Langenberg et al., 2008), morphant CNCCs precociously migrate over the eye (Figs. 5F–I). In addition, after CNCCs have ceased migrating in control embryos, we observe CNCCs in morphant embryos continuing to migrate out over the yolk of the embryo (Figs. 5E, J; arrows in J; Supplementary movies 1 and 2).

We conclude that *cxcr4a* is important for normal CNCC migration into the pharyngeal arches. We do however find that morphants display only a mild migration phenotype as most CNCCs reach the pharyngeal arches. This observation is supported by alcian blue analysis of morphants, which reveals normal ventral craniofacial cartilages in morphant embryos. Moreover, analysis of the pharyngeal arch markers *endothelin-1*, *hand2* and *sox9a* shows that while morphant embryos initially have a delay or reduced expression of these genes, they recover shortly thereafter and have normal arch expression (Supplementary Fig. S3). Conversely, the anterior migration of CNCCs to the presumptive neurocranium may be particularly sensitive to aberrant migration and *cxcr4a*/*sdf1b* levels, resulting in defects within the neurocranium.

cxcr4a and sdf1b overexpression result in CNCC migration defects and ectopic craniofacial cartilages

Loss of *cxcr4a* or *sdf1b* via Morpholino mediated knockdown results in phenotypes in dorsal craniofacial cartilages, but not in the ventral pharyngeal cartilages. *cxcr4a* and *sdf1b* are however expressed in the ventral pharyngeal arches throughout development. We thus asked whether overexpression of either *sdf1b* or *cxcr4a* throughout the embryo would result in phenotypes associated with both viscerocranium and neurocranium development. Although informative, whole embryo overexpression does have some caveats. While we coinject with a fluorescent dextran and screen the embryos for expression, there remains the possibility that the mRNA, and consequently protein, is in fact mosaic. However, we feel that there is sufficient RNA to remain during CNCC migration and early branchial arch patterning, during the time of *sdf1b* and *cxcr4a* function.

Overexpressing *cxcr4a* or *sdf1b* mRNA results in ectopic cartilages, abnormal hyosymplectic elements, unilateral loss of anterior cartilages (Supplementary Fig. S4, arrowheads show *cxcr4a* overexpression), and fusions of ventral pharyngeal cartilages (Supplementary Fig. S4; Supplementary Fig. S5). Embryos injected with either *cxcr4a* or *sdf1b* mRNA have small ectopic cartilages located near the Meckel's and ceratohyal cartilages (Supplementary Figs. S4A, B, D for *cxcr4a*;

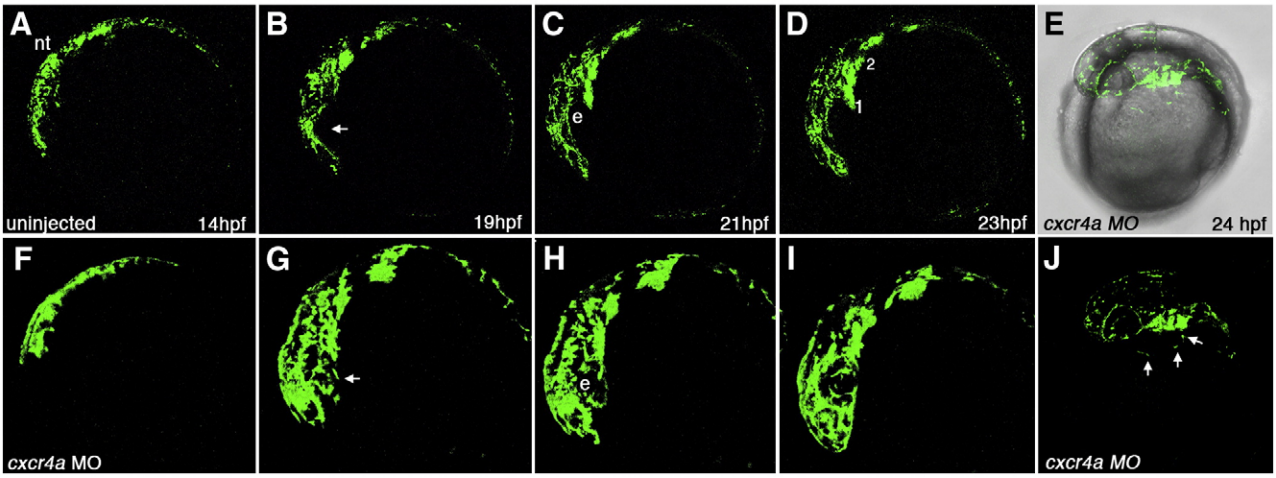

Fig. 5. Time lapse imaging of aberrant CNCC migration in *cxcr4a* morphant embryos. Lateral views, anterior to the left. Stills taken from live time lapse imaging from 14–23 hpf. Wildtype CNCC migration from 14 to 23 hpf (A–D). Wildtype CNCCs avoid the eye during early CNCC migration (B, arrow). *cxcr4a* morphant CNCCs do not avoid the eye during early phases of migration (F–I; B, arrow). (E, J) Brightfield and fluorescent (E) and fluorescence only (J) images of *cxcr4a* morphant CNCCs migrating ectopically over the yolk. e, eye. Numbers denote arches.

Supplementary Fig. S5 for *sdf1b*). Higher doses of *cxcr4a* mRNA (250 pg) cause fusions of the Meckel's and ceratohyal cartilages and less frequently, fusions of the posterior ceratobranchial elements (Supplementary Fig. S4H; arrows). Similarly, *sdf1b* overexpression results in fusions of pharyngeal arch 1 and arch 2 derived skeletal elements (Supplementary Fig. S5C). In addition, the hyosymplectic cartilage is often misshapen or severely reduced in embryos ectopically expressing either *sdf1b* or *cxcr4a* mRNA (Supplementary Fig. S4H; Supplementary Fig. S5C). Taken together, these results suggest that both *sdf1b* and *cxcr4a* play important roles during arch development. Conversely, injection of up to 350 pg of *gfp* mRNA does not result in any craniofacial defects or ectopic cartilages (Supplementary Figs. S4E, G).

Overexpression of *sdf1b* or *cxcr4a* also results in defects within the neurocranium. Lower doses of *cxcr4a* mRNA (100 pg) or *sdf1b* mRNA cause reduction of the trabeculae and a cleft within the ethmoid plate (Supplementary Fig. S4F; Supplementary Fig. S5D). Moreover, ectopic cartilages are often present near the ethmoid plate (Supplementary Fig. S4F; Supplementary Fig. S5D). This phenotype is the opposite of *cxcr4a* morphant larvae, where the ethmoid plate is absent/reduced and the trabeculae are fused and thickened. At higher doses of *sdf1b* or cxcr4a mRNA, however, we find that the ethmoid plate phenotype resembles that of *cxcr4a* and *sdf1b* morphant larvae (data not shown). This suggests that ethmoid plate development is particularly sensitive to the levels of *sdf1b* and *cxcr4a* expression. Similar results have been reported where the overexpression of *sdf1b* mimics the *sdf1b* morphant phenotype in trigeminal ganglion development, as a localized source of Sdf1b is needed for directing migration of cell types (Knaut et al., 2005). In the absence of Sdf1b or in the overexpression of Sdf1b, migrating cells lack a directional cue and are unable to reach their destination.

In order to determine whether these skeletal defects due to ectopic *sdf1b* or *cxcr4a* expression occur early, during migration into the pharyngeal arches, or whether the effects are due to later postmigratory patterning defects, we analyzed the effects of *sdf1b* and *cxcr4a* overexpression on the CNCCs of the pharyngeal arches in tg{sox10::GFP} embryos. We find that ectopic *sdf1b* or *cxcr4a* mRNA results in disorganized arches, with anterior arches often fused (Supplementary Fig. S6C) or reduced (Supplementary Fig. S6B). Posterior arch formation is typically unaltered in embryos overexpressing either *sdf1b* or *cxcr4a*. Significantly, overexpression of either *sdf1b* or *cxcr4a* results in ectopic clusters of CNCCs along the yolk and anteriorly within the head (Supplementary Figs. S6A–D). The presence of ectopic CNCCs throughout the embryo suggests that *sdf1b* and *cxcr4a* overexpression results in CNCC defects during the early stages of pharyngeal arch development that correspond to migration of CNCCs into the arches and the formation of discrete arches.

Ap2a lies upstream of cxcr4a during CNCC development

tfap2a has been shown to be important for neural crest development, survival and for craniofacial cartilage development (Knight et al., 2004, 2005, 2003). We therefore asked whether *cxcr4a* and *sdf1b* expression might be affected in the *tfap2a* mutant *lockjaw* (*low*). At 25 hpf, *sdf1b* and *cxcr7b* expression is normal in *low* mutant embryos (data not shown) suggesting that endoderm formation is unaffected in *low* mutant embryos. We do however find a reduction of *cxcr4a* expression in the pharyngeal region of *low* embryos at 25 hpf (Supplementary Fig. S7). This result is consistent with previous observations that CNCC markers such as *dlx2* (Knight et al., 2003) and *fli1* (Knight et al., 2005) are reduced or absent in *low* mutant embryos.

The bHLH transcription factor *hand2*, a target of endothelin signaling, is expressed in ventral CNCCs during pharyngeal arch development and is required for ventral skeletal cartilage development (Miller et al., 2003; Ruest et al., 2003). We next asked whether *hand2* might regulate *cxcr4a*, *cxcr7b* and *sdf1b* expression. We find that at 25 hpf, han^{S6} mutant embryos display normal *sdf1b*, *cxcr7b* and *cxcr4a* expression, suggesting *hand2* does not regulate *cxcr7b*, *cxcr4a* or *sdf1b* (data not shown). This data is consistent with the observation that early ventral pharyngeal arch markers are unchanged in *hand2* mutant embryos (Miller et al., 2003).

Retinoic acid signaling regulates cxcr7b, cxcr4a and sdf1b expression

In order to ascertain whether RA signaling might regulate *sdf1b*, *cxcr4a* and *cxcr7b* expression, we treated embryos with both RA (100 μM) and the RA synthesis inhibitor DEAB (50 μM) between 21–25 hpf and then examined the expression of *cxcr4a, sdf1b* and *cxcr7b*. Embryos treated with RA have a reduction in the expression of *cxcr4a* and *cxcr7b* (Figs. 6E, G as compared to A, C; arrowheads demarcate the

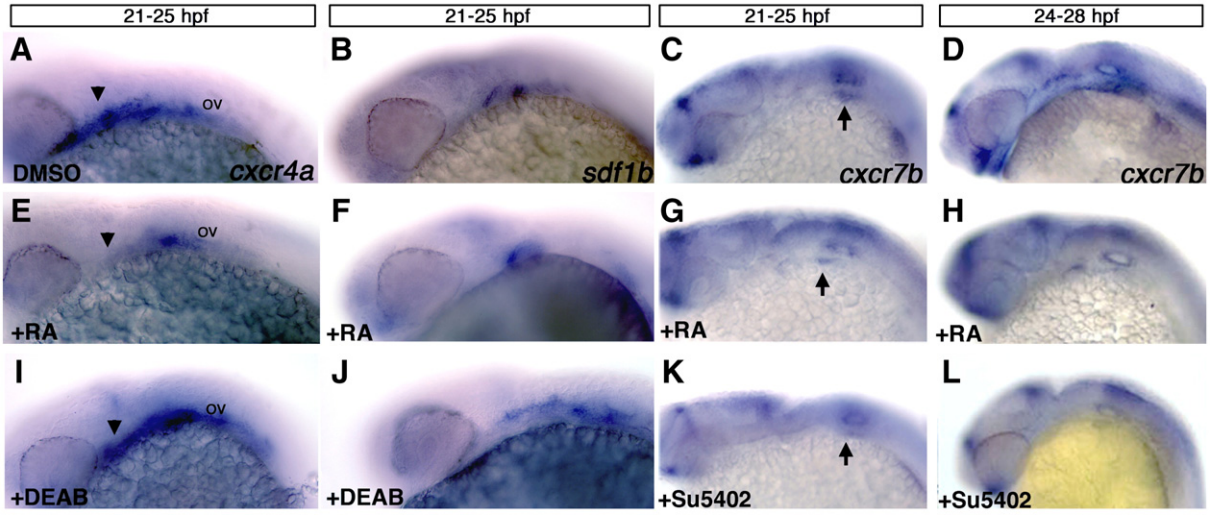

Fig. 6. Retinoic acid signaling is upstream of *cxcr4a* and *sdf1b*. Lateral views, anterior to the left of 25 hpf (A–C, E–G, I–K) and 28 hpf embryos (D, H, L). (A–D) Control embryos treated with DMSO between 21 and 25 hpf show normal expression of *cxcr4a* (A), *sdf1b* (B), and from 21–25 hpf and 24–28 hpf showing normal *cxcr7b* expression (C, D respectively). Embryos treated with 100 μM RA from 21–25 hpf show reduced expression of *cxcr4a* (E as compared to A; arrowheads), a mild reduction in pouch 2 of *sdf1b* (F) and mild reduction of *cxcr7b* (G) below the otic vesicle (arrows point to otic vesicle region in C, G, K). Treatment from 24–28 hpf (H) causes a reduction of *cxcr7b* expression in the endoderm but not the forebrain as compared to wildtype embryos. Embryos treated with the 50 μM RA synthesis inhibitor DEAB show an expansion of *cxcr4a* (I) and *sdf1b* (J) expression posterior to the otic vesicle (ov) as compared to DMSO treated embryos in (A, B). Embryos treated with the Fgf inhibitor Su5402 from 21–25 hpf (K) and 24–28 hpf (L) have reduced expression of *cxcr7b* in the otic region (K, L) and within the pharyngeal endoderm (L) as compared to DMSO treated controls (C, D).

same position in A, E, I as reference, and arrows in C, G, K point to the otic vesicle) and a very slight reduction of *sdf1b* in pouch 2 (Fig. 6F, compared to B). We do not, however, find a change in optic stalk expression of *sdf1b* or *cxcr4a* in response to RA treatment (Figs. 6E, F). The modest decrease in *sdf1b* in response to RA treatment is consistent with previous reports that pharyngeal pouches 1 and 2 are insensitive to RA treatment (Kopinke et al., 2006). Treating embryos with RA from 24–28 hpf also reduces *cxcr7b* expression in the region of the otic vesicle and pharyngeal endoderm but not in the forebrain (Figs. 6D, H).

Embryos treated with DEAB show no effect on *cxcr7b* expression or *sdf1b* and *cxcr4a* expression within the optic stalk (Figs. 6I, J). DEAB treated embryos do, however, have an expansion of both *cxcr4a* and *sdf1b* throughout the pharyngeal arch region (Figs. 6I, J). Moreover, expanded *sdf1b* expression does not take on the normal shape of the pharyngeal endoderm. These results are consistent with previous studies on the effects of DEAB treatment on endodermal pouch morphogenesis, which causes enlargement of endodermal pouches and disrupts posterior pouch formation (Kopinke et al., 2006). Results from our expression analysis in response to RA and DEAB drug treatments suggest that RA signaling lies upstream of *cxcr4a*, *sdf1b* and *cxcr7b* during pharyngeal arch development.

Fgf signaling regulates cxcr7b but not cxcr4a and sdf1b expression

Previous studies have established that Fgf signaling from the pharyngeal endoderm is important for normal arch development (Crump et al., 2004; Piotrowski and Nusslein-Volhard, 2000). We therefore asked whether pharmacological disruption of Fgf signaling would disrupt *sdf1*, *cxcr7b* and *cxcr4* expression. Treating embryos between 21–25 hpf with the Fgf inhibitor SU5402 does not affect *sdf1b* or *cxcr4a* expression, suggesting that Fgf signaling does not regulate *sdf1b* and *cxcr4a* expression (not shown). We do however find that treating embryos with SU5402 between 21–25 hpf does result in decreased expression of *cxcr7b* in the region of the otic placode (Figs. 6C, K). As *cxcr7b* expression commences throughout the pharyngeal region after 28 hpf, we treated embryos with SU5402 from 24–28 hpf and examined expression of *cxcr7b* at 28 hpf. SU5402 treatment between 24–28 hpf results in reduced *cxcr7b* expression in the pharyngeal endoderm (Figs. 6D, L). To ensure that our results were a direct result of Fgf signaling on *cxcr7b* expression and not due to defects in endoderm morphogenesis caused by SU5402 treatment, we treated tg{fli1::eGFP} embryos from 24–28 hpf with SU5402 and visualized the endoderm using the Zn8 antibody. We find that SU5402 treatment at this time period does not result in loss of endodermal pouches. Instead, pouches are slightly misshapen and are not as elongated as DMSO treated control embryos (Supplementary Fig. S8). We conclude that this mild pouch phenotype cannot completely account for the reduction of *cxcr7b* expression. In sum, reduced *cxcr7b* expression is likely due to transcriptional regulation of *cxcr7b* via Fgf signaling.

Hedgehog signaling regulates expression of sdf1b within the optic stalk

Sonic hedgehog (*Shh*) signaling has been shown to be important in the development of the anterior neurocranium and viscerocranial cartilages (Eberhart et al., 2006; Wada et al., 2005). In fact, *shh* mutants and embryos treated with the Hedgehog (Hh) inhibitor cyclopamine have fusion of trabeculae and loss of the ethmoid plate (Wada et al., 2005), similar to *cxcr4a* and *sdf1b* morphants (this study). We treated embryos with cyclopamine throughout development (3 hpf–25 hpf) and examined the expression of *cxcr4a*, *cxcr7b* and *sdf1b*. We find that cyclopamine does not disrupt expression of *cxcr7b* or *sdf1b* within the pharyngeal arches (Figs. 7B, E; data not shown). However, cyclopamine treatment does result in reduced *cxcr4a* expression in the first pharyngeal arch and in mispositioning of the optic stalk (Figs. 7A, D; arrows). Interestingly, cyclopamine treatment also results in loss of *sdf1b* expression in the optic stalk, suggesting that Hh signaling lies upstream of *sdf1b* in the development of the anterior neurocranium (Figs. 7B, E). Thus a possible mechanism of Shh action may in part be mediated by *sdf1b* signaling.

In addition, embryos treated with cyclopamine from 10–24 hpf and subsequently fixed at 28 hpf show lateral line migration defects. Specifically, we find that while *cxcr7b* is still expressed in the lateral line, migration of the lateral line is inhibited (Figs. 7C, F). In control embryos, the lateral line has reached the anterior portion of the yolk sac extension by 28 hpf, while in cyclopamine treated animals, the lateral line lies more anteriorly midway between the otic vesicle and the anterior portion of the yolk sac extension.

Discussion

The results presented in this study highlight a previously undescribed role for chemokine signaling through Sdf1b/Cxcr4a in CNCC migration and in the patterning of CNCC derivatives. Knockdown of Cxcr4a results in aberrant migration of CNCCs to ectopic destinations and in the failure of CNCCs to fully condense within the pharyngeal arches. We hypothesize that the aberrant condensation of CNCCs is due to a role for *cxcr4a*/*sdf1b* in the final steps of CNCC migration. Overexpression of *sdf1b* and *cxcr4a* results in defects in

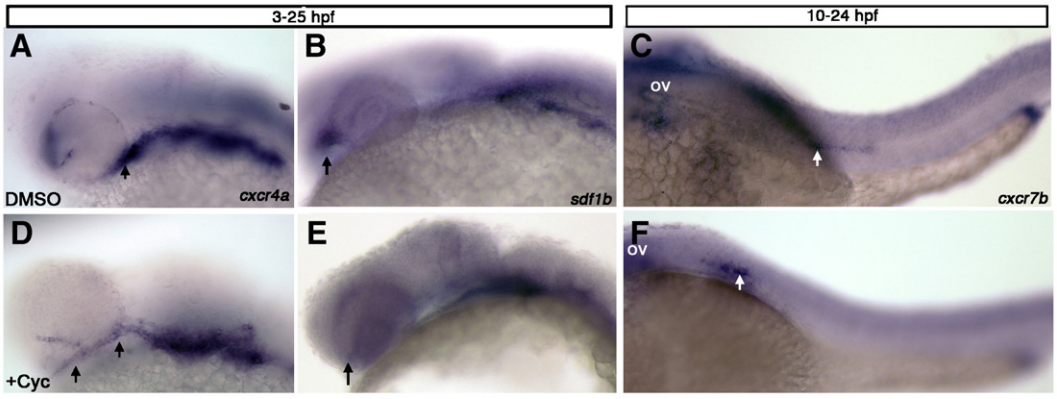

Fig. 7. Hedgehog signaling regulates expression of *sdf1b* within the optic stalk. Lateral views, anterior to the left observed at 25 hpf (A, B, D, E) and 28 hpf (C, F). (A, B) Embryos treated with DMSO or cyclopamine (D, E) from 3 hpf–25 hpf show mispositioned *cxcr4a* expression within the optic stalk and less expression in the first arch of cyclopamine treated embryos (D; arrows), as compared to DMSO treated control embryos (A). *sdf1b* expression in the optic stalk is lost in cyclopamine treated animals (E; arrow) in comparison to DMSO treated controls (B; arrows point to optic stalk in B, E). (C, F) Embryos treated with cyclopamine from 10–24 hpf and observed at 28 hpf with *cxcr7b* expression show lateral line migration defects. The lateral line primordium in cyclopamine treated embryos (F) does not migrate posteriorly as compared to DMSO treated embryos (C; white arrows). ov, otic vesicle.

CNCC migration, pharyngeal arch morphogenesis and patterning of craniofacial cartilage elements. Moreover, both knockdown and overexpression of *sdf1b* and *cxcr4a* leads to migration and craniofacial defects, suggesting that a localized source and strict balance of Sdf1b signaling is required for CNCC migration. Thus, Sdf1b signaling through Cxcr4a functions in the guidance of CNCCs during migration (Knaut et al., 2005; this study). The fact that the CNCCs can reach their final destination suggests that Cxcr4a/Sdf1b signaling is required for directed migration and condensation but not for overall targeting. This hypothesis is consistent with a conserved role for *cxcr4a*/*sdf1b* in directing the migration of a variety of cell types, including mouse DRG and germ cells (Doitsidou et al., 2002; Thorpe et al., 2004; Dumstrei et al., 2004; Knaut et al., 2003; Molyneaux et al., 2003; Belmadani et al., 2005; Sasado et al., 2008).

Interestingly, *cxcr4a* and *sdf1b* expression persists in the pharyngeal arches throughout craniofacial development, after CNCCs have ceased migrating. Additionally, we find that posterior cranial ganglia IX and X are affected in *cxcr4a* morphant embryos suggesting a role for Cxcr4a in patterning the cranial ganglia. While the exact contributions of the CNCCs to the zebrafish cranial ganglia are not known, in chick, the CNCC give rise to both the glossopharyngeal (IX) and vagal (X) cranial ganglia (reviewed by Barlow, 2002). Additionally, craniofacial cartilage phenotypes associated with the overexpression of *cxcr4a* suggest that in addition to being important for migration, *cxcr4a* signaling may also be important for patterning of the craniofacial skeleton. Moreover, while Cxcr7 has been shown to be important in migration of germ cells by helping to establish an Sdf1b gradient (Boldajipour et al., 2008), we find that Cxcr7b does not function with Sdf1/Cxcr4 in CNCC migration and subsequent development of the craniofacial skeleton and ganglia.

A role for Sdf1b/Cxcr4a in CNCC migration

The ability of NCCs to migrate throughout the embryo to reach their final destinations is imperative for the development of multiple structures including craniofacial cartilage and the peripheral nervous system. In the cranial region, CNCC migration is thought to occur by relying on cell–cell communication with each other, as well as with the environment through which they migrate (Kulesa and Fraser, 2000). While work has elucidated the roles of various signaling molecules in the patterning of these NC derivatives, the molecular mechanisms involved in directing NCC migration remain unclear (Clouthier and Schilling, 2004; Yelick and Schilling, 2002). Ephrins and Ephrin receptors have, however, been implicated in regulating CNCC migration and are thought to function by altering cell adhesion, likely through interactions with integrins. In the chick, Ephrin-B1 inhibits NCC migration in the caudal somite and is required for segmental organization of migration (Krull, 1998; Krull et al., 1997). In the mouse embryo, Ephrin-B2 is important for CNCC migration into branchial arch 2, while Ephrin-B1 is required for multiple steps during CNCC migration and mutant mice exhibit a cleft palate (reviewed by Davy and Soriano, 2005). The Neuropilin family has also been shown to be required for NC migration. Knockdown of Neuropilin-1 in chick results in a reduction in the number of CNCCs that reach the branchial arches (McLennan and Kulesa, 2007). Previous studies have also shown that signaling through Neuropilin-2 by Semaphorin 3F is important for proper CNCC migration and condensation of the trigeminal sensory ganglia. Interestingly, while CNCC migration is affected in these mutants, no skeletal defects are apparent (Gammill et al., 2006). *sdf1b* and *cxcr4a* morphants also show aberrant CNCC migration, similar to Neuropilin-2/Semaphorin 3F mutants, but they do not exhibit defects in the viscerocranium, suggesting that most CNCCs are able to reach the arches and become normally patterned. Thus, it is likely that multiple redundant mechanisms are employed to ensure proper craniofacial development.

The results from this study identify a new signaling mechanism that is important for CNCC migration and craniofacial skeleton morphogenesis. We find that Cxcr4a/Sdf1b signaling is important for the migration of CNCCs to the pharyngeal arches and around the eye. *cxcr4a* morphants show aberrant migration of CNCCs across the eye and along the yolk, as well as defects in the condensation of CNCCs into pharyngeal arches. Moreover, overexpression of *cxcr4a* and *sdf1b* results in ectopic migration of CNCCs throughout the anterior embryo.

Recent studies have shown that proper migration of CNCCs around the eye is important for development of the neurocranium (Eberhart et al., 2008; Langenberg et al., 2008). Eberhart et al. (2008) recently described a role for the microRNA Mirn140 in modulating the attraction of CNCCs via platelet derived growth factor (*pdgfaa*) signaling during zebrafish neurocranium development. In embryos lacking Mirn140, CNCCs accumulate around the optic stalk near the attractive Pdgfaa signal and fail to migrate further to the oral ectoderm, resulting in loss of the ethmoid plate and in palatal clefting (Eberhart et al., 2008).

Another study by Langenberg et al. (2008) demonstrated that the eye is important for organizing CNCC migration within the zebrafish embryo. In wild type embryos, CNCCs migrate anteriorly around the eye and are not detected on the eye surface until 23–24 hpf. Soon after, however, CNCCs will cover the surface of the eye. In *chokh(rx3)* mutant embryos that fail to develop eyes, CNCCs do not migrate anteriorly and instead remain disorganized in a region posterior to the normal eye location. Analysis of craniofacial cartilages in *chokh(rx3)* mutant larvae shows loss of the ethmoid plate and fusion of the trabeculae. *chokh(rx3)* mutant larvae do, however, have normal viscerocranium development (Langenberg et al., 2008).

Our results implicate Sdf1b/Cxcr4a signaling in organizing the migration of CNCCs around the eye to the presumptive anterior neurocranium. Loss of *cxcr4a* or overexpression of *sdf1b* results in precocious migration over the surface of the eye, as well as loosely organized pharyngeal arches. Other studies have indicated that Sdf1b signals from the optic stalk to *cxcr4b* expressing retinal ganglion cells and functions in retinal axon guidance (Chalasani et al., 2007; Li et al., 2005).

Thus Sdf1b signaling is important for organizing multiple migratory events around the eye during zebrafish embryonic development.

A role for Cxcr4a/Sdf1b signaling in patterning the craniofacial elements

After neural crest cells have migrated into the branchial arches or anterior optic stalk region, communication between various cell types and tissue layers is paramount to normal patterning of CNCCs (reviewed in Clouthier and Schilling, 2004; Graham and Smith, 2001). Previous reports indicate that the proper formation of endodermal pouches is necessary for craniofacial patterning (Crump et al., 2004; Piotrowski and Nusslein-Volhard, 2000). Moreover, studies regarding the role of the ectoderm in craniofacial development have uncovered the importance of signaling between the ectoderm and CNCCs during craniofacial patterning (Knight et al., 2005; Eberhart et al., 2006). Our analyses of gene expression for *sdf1b* suggest that Sdf1b is secreted from the optic stalk and from the anterior endodermal pharyngeal pouches. This observation, coupled with previous studies that have shown that Sdf1 preferentially binds the Cxcr4 receptor (Horuk, 2001), make it likely that Sdf1b signals from the optic stalk and endoderm to Cxcr4a expressing NCCs to direct migration, craniofacial patterning and morphogenesis. Our hypothesis is supported by the observation that *sdf1b* morphant embryos phenocopy the skeletal defects observed in *cxcr4a* morphants. Our observations further support the idea of crosstalk between tissues, specifically between Sdf1b in the optic stalk and endoderm to Cxcr4a expressing CNCCs during craniofacial development and identify new players in communication between these tissues.

Studies have shown that Fgf and RA signaling are important for patterning the endoderm during craniofacial development. Specifically,

RA and Fgf signaling are dispensable for endoderm specification but have been implicated in regulating endodermal pouch morphogenesis (Crump et al., 2004; Kopinke et al., 2006). We find that RA signaling is important for the regulation of *sdf1b* and *cxcr4a* expression within the pharyngeal arches but not within the optic stalk during zebrafish development. Conversely, we find that Fgf signaling does not regulate *sdf1b*/*cxcr4a* expression.

Analysis of *cxcr4a*/*sdf1b* morphant craniofacial phenotypes with alcian blue staining revealed defects in the neurocranium, including fusion of the tribeculae and loss of the ethmoid plate. These defects phenocopy loss of Hh signaling via the genetic mutant *sonic you* and through pharmacological treatments using the Hh inhibitor cyclopamine (Wada et al., 2005; Eberhart et al., 2006). Hh signaling has been shown to act multiple times during development to initially direct the condensation of CNCCs onto the roof of the stomodeum and later to pattern the neurocranium (Eberhart et al., 2006). The signaling components functioning downstream of Hh in neurocranium development have not, however, been uncovered. We find that *sdf1b* expression within the optic stalk is regulated by Hh signaling. Inhibition of Hh signaling via cyclopamine results in loss of *sdf1b* expression. Taken together, we suggest that *sdf1b* might function downstream of Hh signaling in the development of the anterior neurocranium.

In conclusion, the developmental program that functions to pattern the craniofacial cartilages is a complex process that involves various signaling molecules and communication between various cell types. Here we show that zebrafish chemokine signaling plays a novel role in craniofacial development. Specifically, our data suggests that Sdf1b signaling through the chemokine receptor Cxcr4a is necessary for the condensation of CNCCs into discrete arch structures and in the development of the craniofacial skeleton.

Acknowledgments

We thank L. Hernandez, C. Johnson and D. Killian for discussion and support; M. Singleton for excellent fish care; A. Schier for generously supplying us with the *ody* line; A. Schier, T. Schilling, T. Piotrowski, S. Sperber, I. Dawid and D. Stock for constructs; and M. Wright and C. C. Rossi for double fluorescent *in situ* protocol; L. Niswander and C. Pyrgaki for use of the confocal microscope and advice for live imaging; and D. Clouthier for critical reading of this manuscript. We gratefully acknowledge the support of NIH P30 NS048154 Neuroscience Zebrafish and Imaging Cores, HD050698 and DE017699 to K.B.A, NIH F32 HD056779 to E.O.K. and F32 DE018594 to D.A.B.

Appendix A. Supplementary data

Supplementary data associated with this article can be found, in the online version, at doi:10.1016/j.ydbio.2009.06.031.

References

Ayer-Le Lievre, C.S., Le Douarin, N.M., 1982. The early development of cranial sensory ganglia and the potentialities of their component cells studied in quail-chick chimeras. Dev. Biol. 94, 291–310.

Balabanian, K., Lagane, B., Infantino, S., Chow, K.Y., Harriague, J., Moepps, B., Arenzana-Seisdedos, F., Thelen, M., Bachelerie, F., 2005. The chemokine SDF-1/CXCL12 binds to and signals through the orphan receptor RDC1 in T lymphocytes. J. Biol. Chem. 280, 35760–35766.

Barlow, L.A., 2002. Cranial nerve development: placodal neurons ride the crest. Curr. Biol. 12, R171–R173.

Belmadani, A., Tran, P.B., Ren, D., Assimacopoulos, S., Grove, E.A., Miller, R.J., 2005. The chemokine stromal cell-derived factor-1 regulates the migration of sensory neuron progenitors. J. Neurosci. 25, 3995–4003.

Blentic, A., Tandon, P., Payton, S., Walshe, J., Carney, T., Kelsh, R.N., Mason, I., Graham, A., 2008. The emergence of ectomesenchyme. Dev. Dyn. 237, 592–601.

Bleul, C.C., Fuhlbrigge, R.C., Casasnovas, J.M., Aiuti, A., Springer, T.A., 1996. A highly efficacious lymphocyte chemoattractant, stromal cell-derived factor 1 (SDF-1). J. Exp. Med. 184, 1101–1109.

Boldajipour, B., Mahabaleshwar, H., Kardash, E., Reichman-Fried, M., Blaser, H., Minina, S., Wilson, D., Xu, Q., Raz, E., 2008. Control of chemokine-guided cell migration by ligand sequestration. Cell 132, 463–473.

Brent, A.E., Schweitzer, R., Tabin, C.J., 2003. A somitic compartment of tendon progenitors. Cell 113, 235–248.

Brugmann, S.A., Tapadia, M.D., Helms, J.A., 2006. The molecular origins of species-specific facial pattern. Curr. Top. Dev. Biol. 73, 1–42.

Carney, T.J., Dutton, K.A., Greenhill, E., Delfino-Machin, M., Dufourcq, P., Blader, P., Kelsh, R.N., 2006. A direct role for Sox10 in specification of neural crest-derived sensory neurons. Development 133, 4619–4630.

Chalasani, S.H., Sabol, A., Xu, H., Gyda, M.A., Rasband, K., Granato, M., Chien, C.B., Raper, J.A., 2007. Stromal cell-derived factor-1 antagonizes slit/robo signaling in vivo. J. Neurosci. 27, 973–980.

Chen, J.N., van Bebber, F., Goldstein, A.M., Serluca, F.C., Jackson, D., Childs, S., Serbedzija, G., Warren, K.S., Mably, J.D., Lindahl, P., Mayer, A., Haffter, P., Fishman, M.C., 2001. Genetic steps to organ laterality in zebrafish. Comp. Funct. Genomics 2, 60–68.

Chong, S.W., Emelyanov, A., Gong, Z., Korzh, V., 2001. Expression pattern of two zebrafish genes, cxcr4a and cxcr4b. Mech. Dev. 109, 347–354.

Chong, S.W., Nguyet, L.M., Jiang, Y.J., Korzh, V., 2007. The chemokine Sdf-1 and its receptor Cxcr4 are required for formation of muscle in zebrafish. BMC Dev. Biol. 7, 54.

Clouthier, D.E., Schilling, T.F., 2004. Understanding endothelin-1 function during craniofacial development in the mouse and zebrafish. Birth Defects Res. C. Embryo Today 72, 190–199.

Crump, J.G., Maves, L., Lawson, N.D., Weinstein, B.M., Kimmel, C.B., 2004. An essential role for Fgfs in endodermal pouch formation influences later craniofacial skeletal patterning. Development 131, 5703–5716.

Dambly-Chaudiere, C., Cubedo, N., Ghysen, A., 2007. Control of cell migration in the development of the posterior lateral line: antagonistic interactions between the chemokine receptors CXCR4 and CXCR7/RDC1. BMC Dev. Biol. 7, 23.

Davy, A., Soriano, P., 2005. Ephrin signaling in vivo: look both ways. Dev. Dyn. 232, 1–10.

Doitsidou, M., Reichman-Fried, M., Stebler, J., Koprunner, M., Dorries, J., Meyer, D., Esguerra, C.V., Leung, T., Raz, E., 2002. Guidance of primordial germ cell migration by the chemokine SDF-1. Cell 111, 647–659.

Dumstrei, K., Mennecke, R., Raz, E., 2004. Signaling pathways controlling primordial germ cell migration in zebrafish. J. Cell. Sci. 117, 4787–4795.

Eberhart, J.K., Swartz, M.E., Crump, J.G., Kimmel, C.B., 2006. Early Hedgehog signaling from neural to oral epithelium organizes anterior craniofacial development. Development 133, 1069–1077.

Eberhart, J.K., He, X., Swartz, M.E., Yan, Y.L., Song, H., Boling, T.C., Kunerth, A.K., Walker, M.B., Kimmel, C.B., Postlethwait, J.H., 2008. MicroRNA Mirn140 modulates Pdgf signaling during palatogenesis. Nat. Genet. 40, 290–298.

Gammill, L.S., Gonzalez, C., Bronner-Fraser, M., 2006. Neuropilin 2/semaphorin 3F signaling is essential for cranial neural crest migration and trigeminal ganglion condensation. J. Neurobiol. 67, 47–56.

Graham, A., Smith, A., 2001. Patterning the pharyngeal arches. BioEssays 23, 54–61.

Holzschuh, J., Wada, N., Wada, C., Schaffer, A., Javidan, Y., Tallafuss, A., Bally-Cuif, L., Schilling, T.F., 2005. Requirements for endoderm and BMP signaling in sensory neurogenesis in zebrafish. Development 132, 3731–3742.

Horuk, R., 1998. Chemokines beyond inflammation. Nature 393, 524–525.

Horuk, R., 2001. Chemokine receptors. Cytokine Growth Factor Rev. 12, 313–335.

Huang, X., Saint-Jeannet, J.P., 2004. Induction of the neural crest and the opportunities of life on the edge. Dev. Biol. 275, 1–11.

Kimmel, C.B., Eberhart, J.K., 2008. The midline, oral ectoderm, and the arch-0 problem. Integr. Comp. Biol. 48, 668–680.

Kimmel, C.B., Ballard, W.W., Kimmel, S.R., Ullmann, B., Schilling, T.F., 1995. Stages of embryonic development of the zebrafish. Dev. Dyn. 203, 253–310.

Knaut, H., Werz, C., Geisler, R., Nusslein-Volhard, C., 2003. A zebrafish homologue of the chemokine receptor Cxcr4 is a germ-cell guidance receptor. Nature 421, 279–282.

Knaut, H., Blader, P., Strahle, U., Schier, A.F., 2005. Assembly of trigeminal sensory ganglia by chemokine signaling. Neuron 47, 653–666.

Knight, R.D., Nair, S., Nelson, S.S., Afshar, A., Javidan, Y., Geisler, R., Rauch, G.J., Schilling, T.F., 2003. lockjaw encodes a zebrafish tfap2a required for early neural crest development. Development 130, 5755–5768.

Knight, R.D., Javidan, Y., Nelson, S., Zhang, T., Schilling, T., 2004. Skeletal and pigment cell defects in the lockjaw mutant reveal multiple roles for zebrafish tfap2a in neural crest development. Dev. Dyn. 229, 87–98.

Knight, R.D., Javidan, Y., Zhang, T., Nelson, S., Schilling, T.F., 2005. AP2-dependent signals from the ectoderm regulate craniofacial development in the zebrafish embryo. Development 132, 3127–3138.

Kontges, G., Lumsden, A., 1996. Rhombencephalic neural crest segmentation is preserved throughout craniofacial ontogeny. Development 122, 3229–3242.

Kopinke, D., Sasine, J., Swift, J., Stephens, W.Z., Piotrowski, T., 2006. Retinoic acid is required for endodermal pouch morphogenesis and not for pharyngeal endoderm specification. Dev. Dyn. 235, 2695–2709.

Krull, C.E., 1998. Inhibitory interactions in the patterning of trunk neural crest migration. Ann. N.Y. Acad. Sci. 857, 13–22.

Krull, C.E., Lansford, R., Gale, N.W., Collazo, A., Marcelle, C., Yancopoulos, G.D., Fraser, S.E., Bronner-Fraser, M., 1997. Interactions of Eph-related receptors and ligands confer rostrocaudal pattern to trunk neural crest migration. Curr. Biol. 7, 571–580.

Kucia, M., Jankowski, K., Reca, R., Wysoczynski, M., Bandura, L., Allendorf, D.J., Zhang, J., Ratajczak, J., Ratajczak, M.Z., 2004. CXCR4-SDF-1 signalling, locomotion, chemotaxis and adhesion. J. Mol. Histol. 35, 233–245.

Kulesa, P.M., Fraser, S.E., 2000. In ovo time-lapse analysis of chick hindbrain neural crest cell migration shows cell interactions during migration to the branchial arches. Development 127, 1161–1172.

LaBonne, C., Bronner-Fraser, M., 1998. Induction and patterning of the neural crest, a stem cell-like precursor population. J. Neurobiol. 36, 175–189.

Langenberg, T., Kahana, A., Wszalek, J.A., Halloran, M.C., 2008. The eye organizes neural crest cell migration. Dev. Dyn. 237, 1645–1652.
Lawson, N.D., Weinstein, B.M., 2002. In vivo imaging of embryonic vascular development using transgenic zebrafish. Dev. Biol. 248, 307–318.
Li, Q., Shirabe, K., Thisse, C., Thisse, B., Okamoto, H., Masai, I., Kuwada, J.Y., 2005. Chemokine signaling guides axons within the retina in zebrafish. J. Neurosci. 25, 1711–1717.
McLennan, R., Kulesa, P.M., 2007. In vivo analysis reveals a critical role for neuropilin-1 in cranial neural crest cell migration in chick. Dev. Biol. 301, 227–239.
Miller, C.T., Yelon, D., Stainier, D.Y., Kimmel, C.B., 2003. Two endothelin 1 effectors, hand2 and bapx1, pattern ventral pharyngeal cartilage and the jaw joint. Development 130, 1353–1365.
Miyasaka, N., Knaut, H., Yoshihara, Y., 2007. Cxcl12/Cxcr4 chemokine signaling is required for placode assembly and sensory axon pathfinding in the zebrafish olfactory system. Development 134, 2459–2468.
Mizoguchi, T., Verkade, H., Heath, J.K., Kuroiwa, A., Kikuchi, Y., 2008. Sdf1/Cxcr4 signaling controls the dorsal migration of endodermal cells during zebrafish gastrulation. Development 135, 2521–2529.
Molyneaux, K.A., Zinszner, H., Kunwar, P.S., Schaible, K., Stebler, J., Sunshine, M.J., O'Brien, W., Raz, E., Littman, D., Wylie, C., Lehmann, R., 2003. The chemokine SDF1/CXCL12 and its receptor CXCR4 regulate mouse germ cell migration and survival. Development 130, 4279–4286.
Nair, S., Schilling, T.F., 2008. Chemokine signaling controls endodermal migration during zebrafish gastrulation. Science 322, 89–92.
Pineda, R.H., Svoboda, K.R., Wright, M.A., Taylor, A.D., Novak, A.E., Gamse, J.T., Eisen, J.S., Ribera, A.B., 2006. Knockdown of Nav1.6a Na+ channels affects zebrafish motoneuron development. Development 133, 3827–3836.
Piotrowski, T., Nusslein-Volhard, C., 2000. The endoderm plays an important role in patterning the segmented pharyngeal region in zebrafish (*Danio rerio*). Dev. Biol. 225, 339–356.
Piotrowski, T., Schilling, T.F., Brand, M., Jiang, Y.J., Heisenberg, C.P., Beuchle, D., Grandel, H., van Eeden, F.J., Furutani-Seiki, M., Granato, M., Haffter, P., Hammerschmidt, M., Kane, D.A., Kelsh, R.N., Mullins, M.C., Odenthal, J., Warga, R.M., Nusslein-Volhard, C., 1996. Jaw and branchial arch mutants in zebrafish II: anterior arches and cartilage differentiation. Development 123, 345–356.
Raible, D.W., Wood, A., Hodsdon, W., Henion, P.D., Weston, J.A., Eisen, J.S., 1992. Segregation and early dispersal of neural crest cells in the embryonic zebrafish. Dev. Dyn. 195, 29–42.
Rehimi, R., Khalida, N., Yusuf, F., Dai, F., Morosan-Puopolo, G., Brand-Saberi, B., 2008. Stromal-derived factor-1 (SDF-1) expression during early chick development. Int. J. Dev. Biol. 52, 87–92.
Ruest, L.B., Dager, M., Yanagisawa, H., Charite, J., Hammer, R.E., Olson, E.N., Yanagisawa, M., Clouthier, D.E., 2003. dHAND-Cre transgenic mice reveal specific potential functions of dHAND during craniofacial development. Dev. Biol. 257, 263–277.
Sasado, T., Yasuoka, A., Abe, K., Mitani, H., Furutani-Seiki, M., Tanaka, M., Kondoh, H., 2008. Distinct contributions of CXCR4b and CXCR7/RDC1 receptor systems in regulation of PGC migration revealed by medaka mutants kazura and yanagi. Dev. Biol. 320, 328–339.
Schilling, T.F., Kimmel, C.B., 1994. Segment and cell type lineage restrictions during pharyngeal arch development in the zebrafish embryo. Development 120, 483–494.
Schilling, T.F., Piotrowski, T., Grandel, H., Brand, M., Heisenberg, C.P., Jiang, Y.J., Beuchle, D., Hammerschmidt, M., Kane, D.A., Mullins, M.C., van Eeden, F.J., Kelsh, R.N., Furutani-Seiki, M., Granato, M., Haffter, P., Odenthal, J., Warga, R.M., Trowe, T., Nusslein-Volhard, C., 1996. Jaw and branchial arch mutants in zebrafish I: branchial arches. Development 123, 329–344.
Schwarting, G.A., Henion, T.R., Nugent, J.D., Caplan, B., Tobet, S., 2006. Stromal cell-derived factor-1 (chemokine C-X-C motif ligand 12) and chemokine C-X-C motif receptor 4 are required for migration of gonadotropin-releasing hormone neurons to the forebrain. J. Neurosci. 26, 6834–6840.
Serbedzija, G.N., Fraser, S.E., Bronner-Fraser, M., 1990. Pathways of trunk neural crest cell migration in the mouse embryo as revealed by vital dye labelling. Development 108, 605–612.
Serbedzija, G.N., Bronner-Fraser, M., Fraser, S.E., 1994. Developmental potential of trunk neural crest cells in the mouse. Development 120, 1709–1718.
Sperber, S.M., Dawid, I.B., 2008. barx1 is necessary for ectomesenchyme proliferation and osteochondroprogenitor condensation in the zebrafish pharyngeal arches. Dev. Biol. 321, 101–110.
Svetic, V., Hollway, G.E., Elworthy, S., Chipperfield, T.R., Davison, C., Adams, R.J., Eisen, J.S., Ingham, P.W., Currie, P.D., Kelsh, R.N., 2007. Sdf1a patterns zebrafish melanophores and links the somite and melanophore pattern defects in choker mutants. Development 134, 1011–1022.
Thisse, C. a. T., B. (1998). High resolution whole-mount in situ hybridization. Zebrafish Science Monitor 15, 8–9.
Thisse, B., Pflumio, S., Fürthauer, M., Loppin, B., Heyer, V., Degrave, A., Woehl, R., Lux, A., Steffan, T., Charbonnier, X.Q., Thisse, C., 2001. Expression of the zebrafish genome during embryogenesis. http://zfin.org/cgi-bin/webdriver?MIval=aa-ZDB_home.apg.
Thorpe, J.L., Doitsidou, M., Ho, S.Y., Raz, E., Farber, S.A., 2004. Germ cell migration in zebrafish is dependent on HMGCoA reductase activity and prenylation. Dev. Cell 6, 295–302.
Trainor, P.A., 2005. Specification and patterning of neural crest cells during craniofacial development. Brain Behav. Evol. 66, 266–280.
Trainor, P.A., Krumlauf, R., 2000. Patterning the cranial neural crest: hindbrain segmentation and Hox gene plasticity. Nat. Rev., Neurosci. 1, 116–124.
Ungos, J.M., Karlstrom, R.O., Raible, D.W., 2003. Hedgehog signaling is directly required for the development of zebrafish dorsal root ganglia neurons. Development 130, 5351–5362.
Valentin, G., Haas, P., Gilmour, D., 2007. The chemokine SDF1a coordinates tissue migration through the spatially restricted activation of Cxcr7 and Cxcr4b. Curr. Biol. 17, 1026–1031.
Wada, N., Javidan, Y., Nelson, S., Carney, T.J., Kelsh, R.N., Schilling, T.F., 2005. Hedgehog signaling is required for cranial neural crest morphogenesis and chondrogenesis at the midline in the zebrafish skull. Development 132, 3977–3988.
Westerfield, M., 1993. The Zebrafish Book: A guide for the laboratory use of zebrafish (Danio rerio). University of Oregon Press, Eugene.
Yelick, P.C., Schilling, T.F., 2002. Molecular dissection of craniofacial development using zebrafish. Crit. Rev. Oral Biol. Med. 13, 308–322.